THE JOURNAL OF PHYSICAL CHEMISTRY A

Article

Cite This: J. Phys. Chem. A 2018, 122, 2135−2143

pubs.acs.org/JPCA

Atmospheric Reaction of Cl with 4-Hydroxy-2-pentanone (4H2P): A Theoretical Study

S. Rouichi,[†] S. Samai,[†] A. Ferhati,*[,†] and A. Chakir[‡]

[†]LCCE Laboratoire de Chimie et Chimie de l'Environnement, Faculté des Sciences, Département de Chimie, Université de Batna, 05000 Batna, Algeria

[‡]GSMA, UMR CNRS 6089, UFR Sciences, Université de Reims, BP 1039, 51687 Reims Cedex 2, France

Supporting Information

ABSTRACT: The kinetics and the mechanism of the reaction of 4-hydroxy-2-pentanone (4H2P) with Cl atom were investigated using quantum theoretical calculations. Density functional theory, CBS-QB3, and G3B3 methods are used to explore the reaction pathways. Rice−Ramsperger−Kassel−Marcus theory is employed to obtain rate constants of the reaction at atmospheric pressure and the temperature range 278−400 K. This study provides the first theoretical and kinetic determination of Cl rate constant for reactions with 4H2P over a large temperature range. The obtained rate constant 1.47×10^{-10} cm^3 $molecule^{-1}$ s^{-1} at 298 K is in reasonable agreement with those obtained for C4−C5 hydroxyketones both theoretically and experimentally. The results regarding the structure−reactivity relationship and the atmospheric implications are discussed.

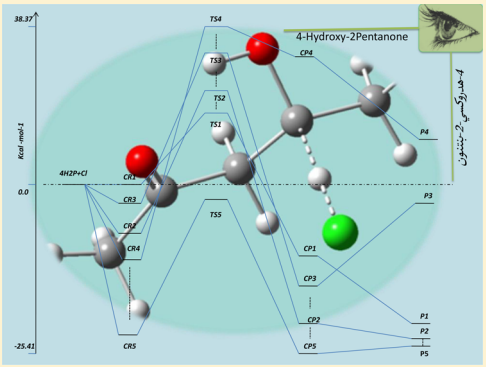

1. INTRODUCTION

Carbonyl compounds play an important role in atmospheric chemistry and in urban air pollution. Ketones, widespread atmospheric key molecular species emitted from both anthropogenic and biogenic sources, are produced in the oxidation of volatile organic compounds (VOCs). They constitute a major class of organics emitted directly into the Earth's troposphere. They are used worldwide in chemistry, in medicine, and in industry as solvents, for resins, lacquers, dyes, flavorings, chloroform, plastics, and for making perfumes and as fuel tracers for monitoring fuel properties. The atmospheric photooxidation of these compounds lead to the formation of organic nitrates and oxygenated products.[1−8]

Hydroxyketones (HKs), secondary products of the reaction of ketones with atmospheric photooxidants in the gas phase, are expected to be removed by chemical reactions with the atmospheric photooxidants (OH, Cl, NO_3, and O_3) and by photolysis. Despite the importance of HKs in atmospheric chemistry, very little information exists concerning their atmospheric fate, in particular, regarding their reaction with Cl atoms.[7] Little information is available in the literature concerning the atmospheric fate of longer chain C4−C5 HKs.[9−13] Three experimental studies report rate constants for chemical reactions of C4−C5 HKs with atmospheric photooxidants[14−18] by using a relative rate technique.[19]

Our work is motivated by the fact that the kinetic studies of the reaction of HK with chlorine radicals are rare in comparison with the kinetic studies of their reaction with OH radicals. So far, it has been carried out by Orlando et al., Stoeffler et al., and Messaadia et al.[20−22]

The chemistry of Cl atoms plays an important role in the troposphere chemistry, particularly in the early morning in sea marsh, continental regions, and in the Arctic troposphere during springtime. Although the peak of Cl atom concentrations (10^3 to 10^4 atoms cm^{-3}) is much lower than that of OH radicals (10^6 atoms cm^{-3}),[8−23] the two reactions can compete with one another in areas where the chlorine atom concentration is sufficiently high because rate constants for the reactions of Cl with organics are generally 10 times higher than the corresponding OH rate constants.[24]

However, very little information exists concerning the atmospheric fate of longer linear chain C4-hydroxyketones toward Cl. Only the gas-phase reactions of 3-hydroxy-2-butanone (3H2B) and 4-hydroxy-2-butanone (4H2B) with Cl investigated in 2013 by Messaadia et al.[13a] can be found in the literature. As many HKs are used as flavors, 4-hydroxy-2-pentanone (4H2P) was mentioned as a biomass-derived compound produced in a significant amount a through different mechanism.[13b]

To the best of our knowledge, there are no theoretical studies concerning the reaction of 4H2P with Cl up to now. The present work reports the first theoretical study regarding the kinetics of the reactions of Cl with 4H2P. The purpose of this work is to provide kinetic data for reactions I−V and to estimate the branching ratios for the different paths contributing to the overall reactions.

Received: December 14, 2017
Revised: January 10, 2018
Published: January 30, 2018

DOI: 10.1021/acs.jpca.7b12291
J. Phys. Chem. A 2018, 122, 2135−2143

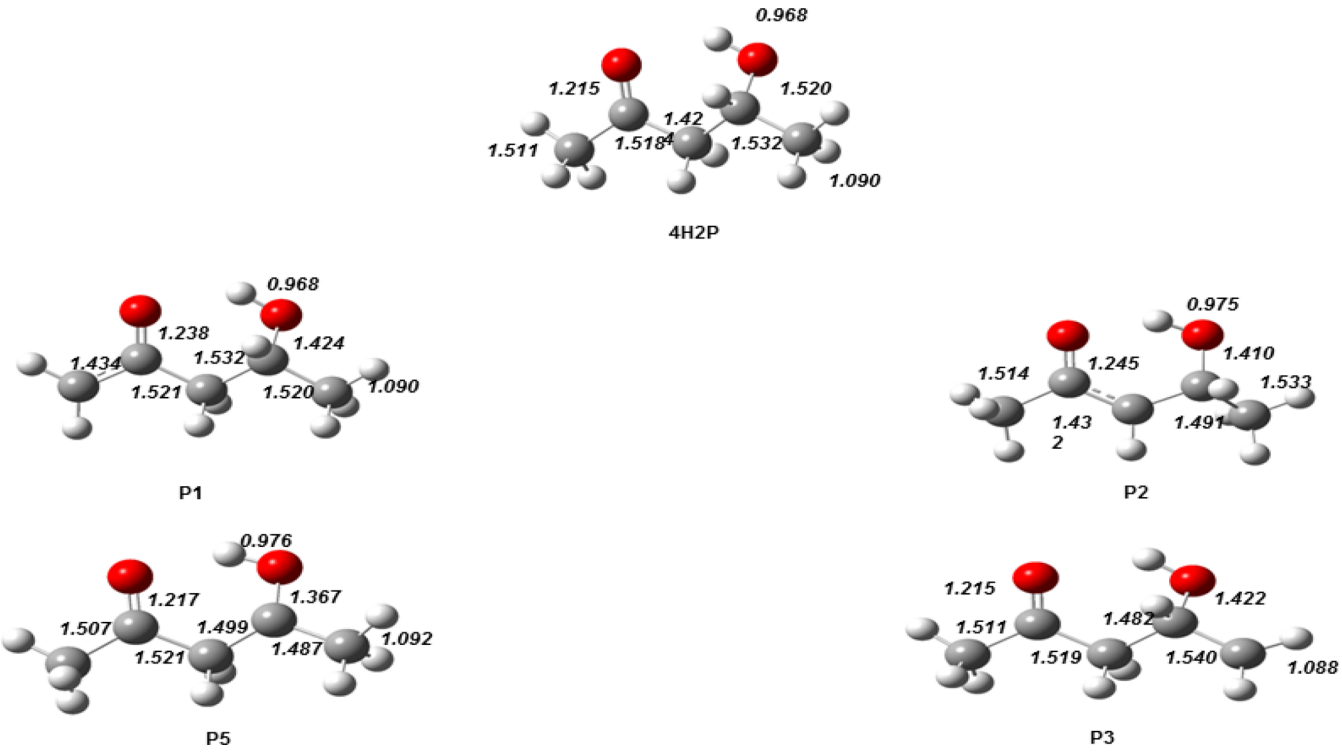

Figure 1. Structures of key species (4H2P (4-hydroxy-2-pentanone) and P1−P5 (radicals obtained via channels I−V)) considered for kinetics simulations determined by B3LYP/6-311++G(2d,pd); bond lengths in angstroms.

$$CH_3COCH_2CHOHCH_3 + Cl \rightarrow \dot{C}H_2COCH_2CHOHCH_3 + HCl \quad (I)$$

$$CH_3COCH_2CHOHCH_3 + Cl \rightarrow CH_3CO\dot{C}H_1CHOHCH_3 + HCl \quad (II)$$

$$CH_3COCH_2CHOHCH_3 + Cl \rightarrow CH_3COCH_2\dot{C}(O)HCH_3 + HCl \quad (III)$$

$$CH_3COCH_2CHOHCH_3 + Cl \rightarrow CH_3COCH_2\dot{C}(OH)CH_3 + HCl \quad (IV)$$

$$CH_3COCH_2CHOHCH_3 + Cl \rightarrow CH_3COCH_2CHOH\dot{C}H_2 + HCl \quad (V)$$

2. THEORETICAL METHODS

2.1. Quantum Chemistry Calculations. Calculations were carried out using Gaussian 09 package[25] available in the CLOVIS platform at the University of Champagne-Ardenne in France. The Optimized geometries and electronic structure for all minima and transitions states have been performed with density functional theory (DFT) B3LYP/6-311++G(2d,pd) level of theory.[26]

The nature of each stationary point was defined by calculating harmonic vibrational frequencies. Every minimum has real frequencies, and the reaction transition states (TSs) are localized by using the procedure "synchronous transit-guided quasi-Newton" for the saddle point search (QST3 in Gaussian 09). The presence of a single negative frequency in the Hessian matrix of TSs is always controlled. Animation of the imaginary frequency, often combined with intrinsic reaction coordinate (IRC) calculations,[27] enabled us to correlate a certain transition structure explicitly with its reactants and products.

The B3LYP method overestimates hydrogen-abstraction reaction energies[28−38] and hence gives unreliable thermochemical predictions. Therefore, in this work, B3LYP method was used only to optimize neutrals, radicals, and transition-states geometries, whereas the CBS-QB3 model of Petersson and coworkers[38] was used to compute the energies of the different systems studied here. In fact, recent studies indicate that the CBS-QB3 method often provides good agreement with experimental reaction energies and barriers for molecules having similar size as those studied in this work.[39−41] It should be noted that the energies of all structures were obtained using the CBS-QB3 method, and differences in zero-point vibrational energies scaled by 0.99 were corrected for.[28] Moreover, the study by Dybala-Defratyka et al.[42] suggests that errors in CBS-QB3 atomization energies are <4 kcal/mol.

Radom and coworkers[43] have revealed that for the standard CBS-QB3 method a correction for spin-contamination in open-shell species must be added to the total energy. Heat of formation for all gaseous species involved in the reaction was calculated based on the procedure described in the literature.[39,44]

G3B3 (or G3//B3LYP) is a variant of G3 method, in which structures and zero-point vibrational energies are calculated at the B3LYP/6-31G(d) level. This is advantageous for larger open-shell systems showing spin contamination. The mean absolute deviation for the neutral set of molecule is ∼1 kcal/mol[45]

The CBS-QB3 and G3B3, two methods that utilize B3LYP geometries instead of UMP2 ones, and, as mentioned above, the B3LYP geometries have been shown to be accurate[46]

DOI: 10.1021/acs.jpca.7b12291
J. Phys. Chem. A 2018, 122, 2135−2143

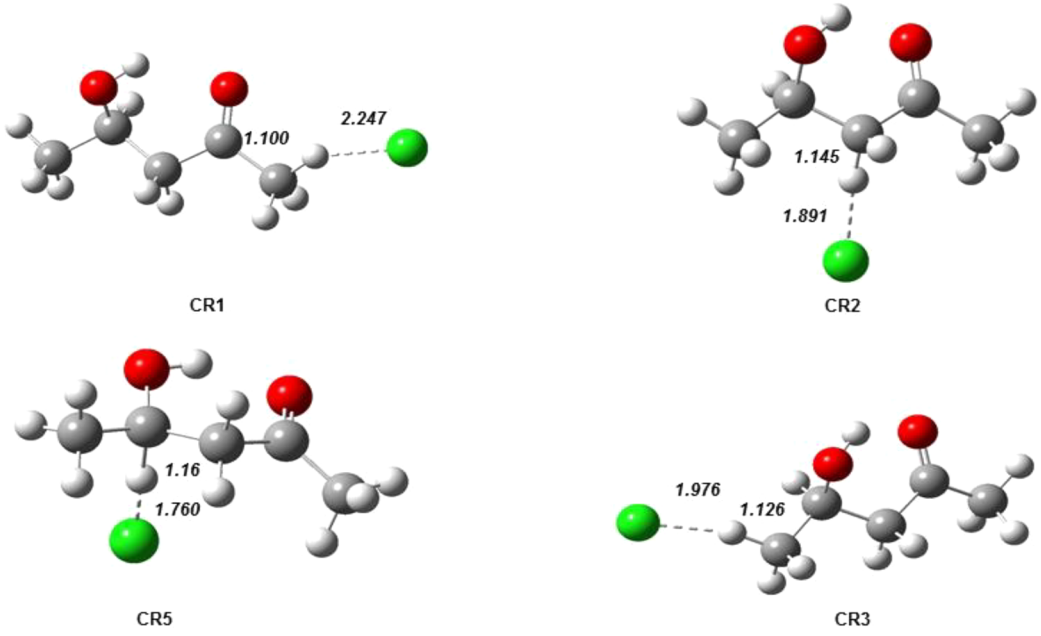

Figure 2. Structures of key species CR1−CR5 (radicals obtained via channels I−V) considered for kinetics simulations determined by B3LYP/6-311++G(2d,pd); bond lengths in angstroms.

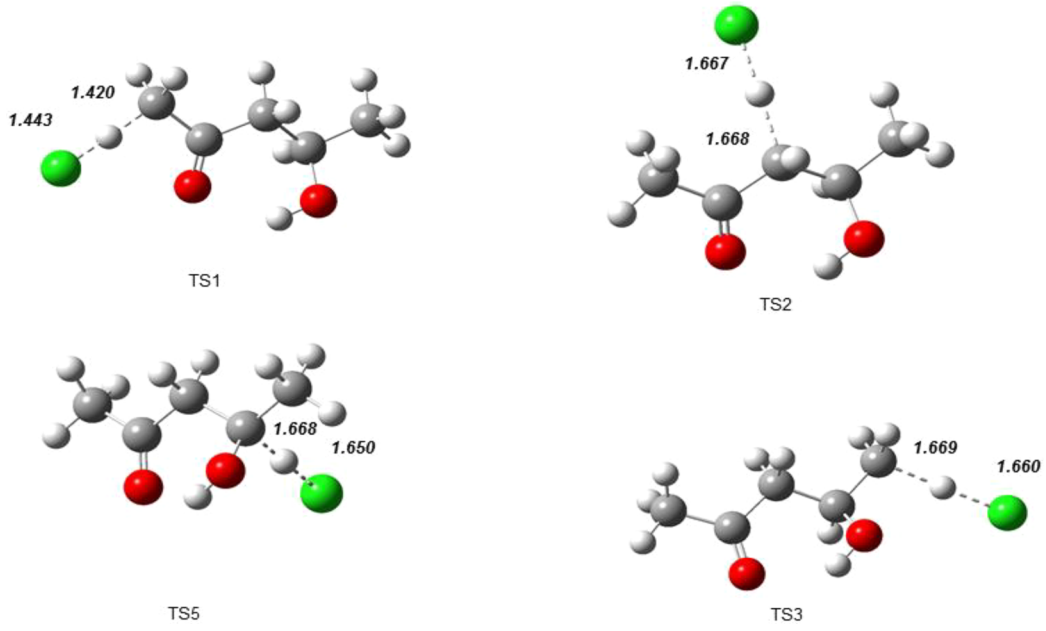

Figure 3. Structures of key species TS1−TS5 (radicals obtained via channels I−V) considered for kinetics simulations determined by B3LYP/6-311++G(2d,pd); bond lengths in angstroms.

Theoretical enthalpies of formation at 0 K and theoretical enthalpies of formation at 298 K are calculated as described in our previous work.[47,48]

2.2. Rate Theory Calculations. The rate constants reaction were obtained using RRKM (Rice−Ramsperger−Kassel−Marcus) theory[49−52] with the required sums, density of states, frequencies, zero-point energies, moments of inertia, and symmetries. Kinetic behaviors of the reaction were obtained from optimized reactants, TSs, and products at B3LYP/6-311++G(2d,pd) level of theory. Theoretical enthalpies obtained from both CBS-QB3//B3LYP/6-311++G(2d,pd) and G3B3//B3LYP/6-311++G(2d,pd) calculations for all gaseous species involved in the reaction were introduced in the CHEMRATE database.

The calculations were done to determine the temperature dependence of each reaction involved in the mechanism. Further details of the time-dependent master equation (ME) analysis in CHEMRATE are accessible in the literatures.[49−52] The precision of the method implemented in CHEMRATE was found to be sufficient through wide comparison with experimental and theoretical data.[53−55] We did not take into account the low-frequency internal rotations as hindered rotors; our simulations take only the most stable conformer. These simplifications will have small influence on numerical accuracy but should not deviate from the validity of rates values.

DOI: 10.1021/acs.jpca.7b12291
J. Phys. Chem. A 2018, 122, 2135−2143

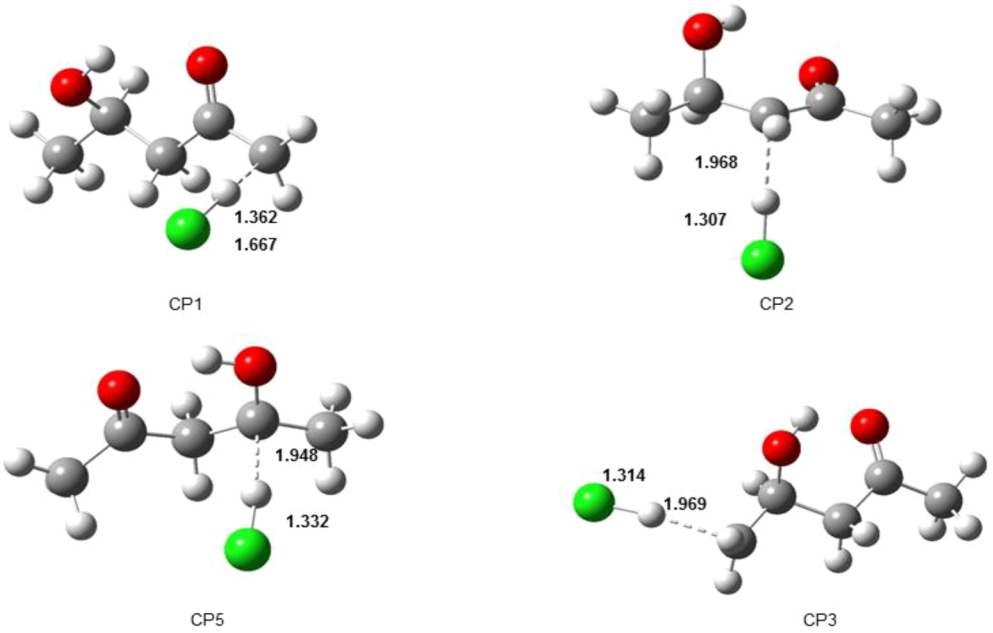

Figure 4. Structures of key species CP1−CP5 (radicals obtained via channels I−V) considered for kinetics simulations determined by B3LYP/6-311++G(2d,pd); bond lengths in angstroms.

Table 1. Energies of Reactants and Products Species Involved in the Mechanism Obtained at CBS-QB3//B3LYP/6-311G++(2d,pd) Level: CBS-H Enthalpy at 2 98.15 K. CBS-G Gibbs Free Energy at 298.15 K. CBS-E Energy.CBS (0 K) Energy at 0 K.

	CBS-H	CBS-G	CBS-E	CBS (0 K)	$\Delta_f H°_{0K}$ [a]	$D_0°$ [b]	$\Delta_f H°_{298K}$ [c]	ΔH_r(298 K) [d]	ΔG_r(298 K) [f]	img freq [g]
4H2P+CL	−806.093445	−806.154282	−806.095334	−806.105352	−323.23	1836.00	−330.28	0.00	0.00	
CR1	−806.093613	−806.144258	−806.094557	−806.105288	−323.18	1835.95	−330.39	−0.11	6.29	
CR2	−806.097605	−806.148516	−806.098549	−806.109497	−325.83	1838.60	−332.89	−2.61	3.62	
CR3	−806.095216	−806.147282	−806.096160	−806.107225	−324.40	1837.17	−331.39	−1.11	4.39	
CR4	−806.099755	−806.149388	−806.100699	−806.111516	−327.09	1839.86	−334.24	−3.96	3.07	
CR5	−806.118296	−806.167182	−806.119240	−806.129687	−338.50	1851.27	−345.88	−15.59	−8.09	
TS1	−806.085777	−806.135066	−806.086721	−806.096925	−317.94	1830.71	−325.47	4.81	12.06	−1108.13
TS2	−806.075320	−806.124752	−806.076265	−806.086904	−311.65	1824.42	−318.91	11.37	18.53	−1781.9
TS3	−806.069538	−806.118543	−806.070482	−806.080893	−307.88	1820.65	−315.28	15.00	22.43	−1839.37
TS4	−806.032456	−806.078640	−806.033400	−806.042991	−284.09	1796.86	−292.01	38.27	47.47	−723.0
TS5	−806.094881	−806.143888	−806.095825	−806.106393	−323.88	1836.65	−331.18	−0.90	6.52	−1511.24
CP1	−806.099467	−806.140423	−806.099469	−806.110328	−326.35	1839.12	−334.06	−3.78	8.70	
CP2	−806.114374	−806.154512	−806.114373	−806.126980	−336.80	1849.57	−343.42	−13.13	−0.14	
CP3	−806.104532	−806.145596	−806.104532	−806.116427	−330.17	1842.94	−337.24	−6.96	5.45	
CP4	−806.066057	−806.112797	−806.067001	−806.076879	−305.36	1818.13	−313.10	17.19	26.03	
CP5	−806.133946	−806.172031	−806.133945	−806.145337	−348.32	1861.09	−355.70	−25.41	−11.14	
P1	−806.105920	−806.169564	−806.107808	−806.118395	−331.41	1844.18	−338.11	−7.83	−9.59	
P2	−806.108775	−806.173719	−806.107808	−806.118395	−331.41	1844.18	−339.90	−9.62	−12.20	
P3	−806.094685	−806.160097	−806.096573	−806.107900	−324.82	1837.59	−331.06	−0.78	−3.65	
P4	−806.084667	−806.149925	−806.086556	−806.097519	−318,.31	1831.08	−324.78	5.51	2.73	
P5	−806.109771	−806.174514	−806.111660	−806.122634	−334.07	1846.84	−340.53	−10.24	−12.70	

[a]Heat of formation at 0 K in kcal mol^{-1}. [b]Atomization energy in kcal mol^{-1} at 0 K. [c]Heat of formation at 298.15 K in kcal mol^{-1}. [d]Enthalpy of reaction at 298.15 K in kcal mol^{-1}. [f]Gibbs energy of reaction at 298.15 K in kcal mol^{-1}. [g]Imaginary frequencies for TSs.

3. STRUCTURAL CALCULATIONS

The calculation involves an examination of the H- abstraction from 4H2P. The reaction is expected to proceed via H abstraction from the ($CH_3C(O)-$), $-CH_2-$, CH(OH)−, or $-CH_3$ groups. The TSs are characterized by a near-linear alignment of the Cl atom, the hydrogen to be abstracted, and the central atom of abstraction. The different H-abstraction paths proceed via three steps. In the first step, the radical approaches the H atom to be abstracted of the 4H2P, forming an intermediate complex (CR: complex reactant) more energetically stable than the reactants. In the second step of the reaction the intermediate complex dissociates to form an intermediate complex (CP: complex product) through a TS (Figures 1−4). The H abstractions, from ($CH_3C(O)-$), $-CH_2-$, CH(OH)−, and $-CH_3$ groups, were found to be exothermic and exoergonic for 4H2P with Cl at the CBS-QB3//B3LYP/6-311++G(2d,pd) level of theory. At the G3B3//B3LYP/6-311++G(2d,pd) level, the H abstractions, from $-CH_3$ group adjacent to the −CH(OH) group, are endothermic and endoergonic. The energies of all species

DOI: 10.1021/acs.jpca.7b12291
J. Phys. Chem. A 2018, 122, 2135−2143

Table 2. Energies of Reactants and Products Species Involved in the Mechanism Obtained at G3B3//B3LYP/6-311G++(2d,pd) Level: CBS-H Enthalpy at 2 98.15 K. CBS-G Gibbs Free Energy at 298.15 K. CBS-E eEnergy.CBS (0 K) Energy at 0 K.

	G3B3-H	G3B3-G	G3B3-E	G3B3 (0 K)	$\Delta_f H°_{0K}$ [a]	$D_0°$ [b]	$\Delta_f H°_{298K}$ [c]	ΔH_r(298 K) [d]	ΔG_r(298 K) [e]	img freq [f]
4H2P+CL	−806.721303	−806.782531	−806.723192	−806.733398	−316.31	1829.08	−323.26	0.00	0.00	
CR1	−806.721281	−806.772373	−806.722225	−806.733156	−316.16	1828.93	−323.24	0.01	6.37	
CR2	−806.723682	−806.775046	−806.724627	−806.735774	−317.81	1830.58	−324.75	−1.49	4.70	
CR3	−806.721782	−806.774300	−806.722726	−806.733986	−316.68	1829.45	−323.56	−0.30	5.17	
CR4	−806.726818	−806.776903	−806.727762	−806.738781	−319.69	1832.46	−326.72	−3.46	3.53	
CR5	−806.740482	−806.789817	−806.741427	−806.752084	−328.04	1840.81	−335.29	−12.04	−4.57	
TS1	−806.709395	−806.759129	−806.710339	−806.720758	−308.38	1821.15	−315.78	7.47	14.68	−1108.13
TS2	−806.699506	−806.749390	−806.700450	−806.711298	−302.45	1815.22	−309.58	13.68	20.80	−1781.9
TS3	−806.693043	−806.742495	−806.693987	−806.704608	−298.25	1811.02	−305.52	17.73	25.12	−1839.37
TS4	[g]	[g]	[g]	[g]	[g]	[g]	[g]	[g]	[g]	−723.0
TS5	−806.717818	−806.767277	−806.718762	−806.729540	−313.89	1826.66	−321.07	2.19	9.57	−1511.24
CP1	−806.725284	−806.778050	−806.726228	−806.737172	−318.68	1831.45	−325.75	−2.50	2.81	
CP2	−806.734875	−806.787908	−806.735820	−806.747759	−325.33	1838.10	−331.77	−8.52	−3.37	
CP3	−806.723412	−806.777142	−806.724356	−806.736186	−318.06	1830.83	−324.58	−1.32	3.38	
CP4	−806.726818	−806.776903	−806.727762	−806.738781	−319.69	1832.46	−326.72	−3.46	3.53	
CP5	−806.744881	−806.796762	−806.745826	−806.757215	−331.26	1844.03	−338.05	−14.80	−8.93	
P1	−806.731684	−806.795685	−806.733572	−806.744346	−323.18	1835.95	−329.77	−6.51	−8.25	
P2	−806.734084	−806.799380	−806.735972	−806.746989	−324.84	1837.61	−331.28	−8.02	−10.57	
P3	−806.720960	−806.786750	−806.722849	−806.734360	−316.92	1829.69	−323.04	0.22	−2.65	
P4	−806.710883	−806.776493	−806.712771	−806.723907	−310.36	1823.13	−316.72	6.54	3.79	
P5	−806.735202	−806.800301	−806.737090	−806.748238	−325.63	1838.40	−331.98	−8.72	−11.15	

[a]Heat of formation at 0 K in kcal mol^{-1}. [b]Atomization energy in kcal mol-1 at 0 K. [c]Heat of formation at 298.15 K in kcal mol^{-1}. [d]Enthalpy of reaction at 298.15 K in kcal mol^{-1}. [e]Gibbs energy of reaction at 298.15 K in kcal mol^{-1}. [f]Imaginary frequencies for TSs. [g]For G3B3, TS4 calculation encountered convergence problems.

involved in the H-abstraction reaction are reported in Tables 1 and 2 for 4H2P+Cl.

3.1. Path 1 Abstraction from Group CH_3CO-. This path starts from the reactant complex CR1 toward the complex product CP1, which includes a strong intermolecular hydrogen interaction between the carbon radical site of the CH_3CO group and H−Cl with a bond distance of 1.667 Å. The bond distance C−H in the reactant complex CR1 is ∼1.100 Å, the like bond H···Cl distance is ∼2.247 Å, while in the transition TS1, the same bond distances are, respectively, ∼1.420 and ∼1.443 Å. The product complex CP1 gives rise to radical P1 and HCl. The reaction process is exothermic and exoergonic and involves an energy barrier of ∼12.06(*14.68*) kcal/mol with reaction enthalpy of ∼7.83(*6.51*) kcal/mol and Gibbs free energy of ∼9.59(*8.25*) kcal/mol (italics in parentheses represent the energy barrier at G3B3//B3LYP/6-311++G-(2d,pd) level)

3.2. Path 2 Abstraction from Group $-CH_2-$. The H-abstraction process in this path concerns one hydrogen of the C−H bonds of the $-CH_2-$ group adjacent to the carbonyl of the 4H2P. The product complex CP2 includes an intermediate intermolecular hydrogen bond between the carbon radical site of the $-CH_2-$ group and HCl with a bond distance of ∼1.968 Å. The bond distance C−H in the reactant complex CR2 is ∼1.145 Å, the like bond H···Cl distance is ∼1.891 Å, while in the transition TS2 the same bonds distances are, respectively, ∼1.668 and ∼1.667 Å. The product complex CP2 by dissociation of the hydrogen intermolecular bond gives rise to product P2 and HCl. The reaction process is also exothermic and exergonic. This reaction involves a transition state TS2 with energy barrier of ∼18.53(20.80) kcal/mol with reaction enthalpy of ∼9.62(8.02) kcal/mol and Gibbs free energy of ∼12.20(10.57) kcal/mol.

3.3. Path 3 Abstraction from Group $-CH_3$. The H abstraction initiated in this path involves one hydrogen of the C−H bonds of the $-CH_3$ group adjacent to the −CH(OH) group. The bond distance C−H in the reactant complex CR3 is 1.126 A and C−H···Cl intermediate hydrogen bond is ∼1.976 Å, while for the transition TS3, the same bonds distances are, respectively, ∼1.669 and ∼1.660 Å. The product complex CP3 includes an intermolecular H bond between the carbon radical site and HCl with a bond distance of ∼1.969 Å. The product complex CP3 gives rise to product P3 and HCl. This reaction involves an energy barrier of ∼22.43(25.12) kcal/mol with reaction enthalpy of ∼0.70(−0.22) kcal/mol and Gibbs free energy of ∼3.65(2.65) kcal/mol. The reaction process is slightly exothermic and exoergonic.

3.4. Path 4 Abstraction from Group −CH(OH)−. For the path involving abstraction of the hydrogen of the hydroxyl from group CH(OH), calculation gives a very high barrier TS4 ∼47.5 kcal/mol (for the G3B3 level, calculation optimization of the TS encountered convergence problems) compared with the other paths was not considered in the kinetic calculations. The H abstractions are endothermic ∼5.51(6.54) kcal/mol and endoergonic ∼2.73(3.79)kcal/mol. It is important to note that all species optimized in this study involve a six-member-like cycle with a H bond between the hydrogen of the hydroxyl and the carbonyl groups (∼1.820 Å). In the study of Priya and coworkers,[19] the same difficulties, although at low-level theory, were encountered to optimize structures for abstraction from the hydroxyl group path, probably to high barrier energies, unreachable TSs, and convergence calculations problems.

3.5. Path 5 Abstraction from Group −CH(OH)−. In this path, the unique hydrogen involved in the process of H abstraction is the H atom in the C−H bond of the −CH(OH)− group of 4H2P. The bond distance C−H in the reactant complex CR5 is ∼1.116 Å and the C−H···Cl strong hydrogen bond is ∼1.760 Å, while for the transition TS5 the same bonds distances are, respectively, ∼1.668 and ∼1.650 Å. This reaction involves an energy barrier of ∼6.52(9.57) kcal/

DOI: 10.1021/acs.jpca.7b12291
J. Phys. Chem. A 2018, 122, 2135−2143

Table 3. Rate Constants (cm^3 $molecule^{-1}$ s^{-1}) and Branching Ratio ($\beta 4$) within the Temperature Range 278−400 K for Reaction 4H2P + Cl at CBS-QB3//B3LYP/6-311G++(2d,pd) Level. β_V Is the Branching Ratio of the Majority Channel.

T (K)	K_I	K_{II}	K_{III}	K_V	K	β_V
278	3.53×10^{-32}	1.73×10^{-18}	3.54×10^{-27}	9.46×10^{-11}	9.46×10^{-11}	0.999
298	9.02×10^{-31}	8.61×10^{-18}	7.68×10^{-26}	1.47×10^{-10}	1.47×10^{-10}	0.999
315	1.02×10^{-29}	2.73×10^{-17}	7.33×10^{-25}	1.96×10^{-10}	1.96×10^{-10}	0.999
334	1.13×10^{-28}	8.20×10^{-17}	6.60×10^{-24}	2.47×10^{-10}	2.47×10^{-10}	0.999
356	1.32×10^{-27}	2.39×10^{-16}	5.89×10^{-23}	2.95×10^{-10}	2.95×10^{-10}	0.999
381	1.51×10^{-26}	6.53×10^{-16}	4.86×10^{-22}	3.30×10^{-10}	3.30×10^{-10}	0.999
400	7.86×10^{-26}	1.24×10^{-15}	1.94×10^{-21}	3.43×10^{-10}	3.43×10^{-10}	0.999

Table 4. Rate Constants (cm^3 $molecule^{-1}$ s^{-1}) and Branching Ratio ($\beta 4$) within the Temperature Range 278−400 K for Reaction 4H2P + Cl at G3B3//B3LYP/6-311G++(2d,pd) Level. β_V Is the Branching Ratio of the Majority Channel.

T (K)	K_I	K_{II}	K_{III}	K_V	K	β_V
278	3.23×10^{-27}	8.57×10^{-20}	3.19×10^{-26}	6.25×10^{-14}	6.25×10^{-14}	0.999
298	4.22×10^{-26}	5.58×10^{-19}	$6,65 \times 10^{-25}$	1.57×10^{-13}	1.57×10^{-13}	0.999
315	2.82×10^{-25}	2.16×10^{-18}	6.17×10^{-24}	2.97×10^{-13}	2.97×10^{-13}	0.999
334	1.84×10^{-24}	7.93×10^{-18}	5.39×10^{-23}	5.34×10^{-13}	5.34×10^{-13}	0.999
356	1.23×10^{-23}	2.83×10^{-17}	4.67×10^{-22}	9.20×10^{-13}	9.20×10^{-13}	0.999
381	8.06×10^{-23}	9.39×10^{-17}	3.72×10^{-21}	1.48×10^{-12}	1.48×10^{-12}	0.999
400	2.84×10^{-22}	2.03×10^{-16}	1.44×10^{-20}	1.97×10^{-12}	1.97×10^{-12}	0.999

mol with reaction enthalpy of ∼10.24(8.72) kcal/mol and Gibbs free energy of ∼12.70(11.15) kcal/mol. The product complex CP5, which gives rise to product P3 and HCl, includes an intermolecular bond between the carbon radical site of the −CH(OH)− group and HCl with a like bond distance of ∼1.942 Å.

4. KINETICS

The mechanism of H-abstraction reaction of 4H2P with Cl is examined as a competition between four H abstractions as follows

$$4H2P + X \underset{\overleftarrow{k}_{-Ia}}{\overrightarrow{k}_{Ia}} (CR)_I \xrightarrow{\overrightarrow{k}_{Ib}} (CP)_I \underset{\overleftarrow{k}_{-Ic}}{\overrightarrow{k}_{Ic}} P1 + HCl$$

$$4H2P + X \underset{\overleftarrow{k}_{-IIa}}{\overrightarrow{k}_{IIa}} (CR)_{II} \xrightarrow{\overrightarrow{k}_{IIb}} (CP)_{II} \underset{\overleftarrow{k}_{-IIc}}{\overrightarrow{k}_{IIc}} P2 + HCl$$

$$4H2P + X \underset{\overleftarrow{k}_{-IIIa}}{\overrightarrow{k}_{IIIa}} (CR)_{III} \xrightarrow{\overrightarrow{k}_{IIIb}} (CP)_{III} \underset{\overleftarrow{k}_{-IIIc}}{\overrightarrow{k}_{IIIc}} P3 + HCl$$

$$4H2P + X \underset{\overleftarrow{k}_{-Va}}{\overrightarrow{k}_{Va}} (CR)_V \xrightarrow{\overrightarrow{k}_{Vb}} (CP)_V \underset{\overleftarrow{k}_{-Vc}}{\overrightarrow{k}_{Vc}} P4 + HCl$$

According to the reaction profiles, the rate constant (k) resultant to all of the studied reaction channels can be analyzed in terms of conventional transition-state theory (TST) or RRKM/ME calculations. k_{Ia}, k_{IIa}, k_{IIIa}, and k_{Va} are the forward rates and k_{-Ia}, k_{-IIa}, k_{-IIIa}, and k_{-Va} are reverse ones for the first step and k_{Ib}, k_{IIb}, k_{IIIb}, and k_{Vb} correspond to the second steps, respectively, for channels I−V. k_{Ic}, k_{IIc}, k_{IIIc}, and k_{Vc} are the forward rates and k_{-Ic}, k_{-IIc}, k_{-IIIc}, and k_{-Vc} are the reverse ones for the last step. On the basis of this hypothesis, rate constants of channels I−V (k_I, k_{II}, k_{III}, and k_V) can be expressed as

$$k_I = k_{eqIa} \times k_{Ib} \times k_{eqIc} \quad (a)$$

$$k_{II} = k_{eqIIa} \times k_{IIb} \times k_{eqIIc} \quad (b)$$

$$k_{III} = k_{eqIIIa} \times k_{IIIb} \times k_{eqIIIc} \quad (c)$$

$$k_V = k_{eqVa} \times k_{Vb} \times k_{eqVc} \quad (d)$$

where k_{eq} (eqs a−d) are the equilibrium constants between the isolated reactants and the products for channel I to channel V, respectively. All rate constants involved in the H-abstraction reaction mechanism were calculated with ChemRate program.[29] Simulations were performed at pressure of 1 atm and temperature range 278−400 K. Collisional energy transfer was described using an exponential-down model, with ΔE_{down} = 300 cm^{-1} and Ar as a bath gas with Lennard-Jones parameters of σ = 4.4 and ξ = 216 K.[56,57] All rate constants quoted in this study are in s^{-1} or cm^3 $molecule^{-1}$ s^{-1} units.

In this case, the overall rate constant (eq e) and the branching ratios (eq f) obtained from theoretical kinetic simulation are calculated as follows

$$k = k_I + k_{II} + k_{III} + k_V \quad (e)$$

$$\beta_I = \frac{k_I}{k_I + k_{II} + k_{III} + k_V} \quad \text{and} \quad \beta_I = 1 - (\beta_{II} + \beta_{III} + \beta_V) \quad (f)$$

5. RESULTS AND DISCUSSION

The dominant mechanistic channel of the reaction of 4H2P with Cl involves the abstraction of H atom from the CH(OH)− group (as attended), which proceeds through the TS3 transition state with branching ratio βI of ∼99% in the temperature range 278−400 K. For the H abstraction from the CH_2, CH_3CO, and CH_3 groups, rate constants values are negligible relative to k_V (Table 3 and 4). Significant positive temperature dependence is observed for k. The linear least-square fit of all data points is provided by the calculation at different temperatures leads, with a correlation coefficient of ∼0.999, to the following Arrhenius expressions in cm^3 $molecule^{-1}$ s^{-1} at CBS-QB3 (eq g) and G3B3 (eq h) level of theory, respectively

DOI: 10.1021/acs.jpca.7b12291
J. Phys. Chem. A 2018, 122, 2135−2143

$$k(T) = 7.29 \times 10^{-9} * \exp(-1166/T) \quad \text{(g)}$$

$$k(T) = 5.77 \times 10^{-9} * \exp(-3137/T) \quad \text{(h)}$$

The calculations of the transmission coefficients, using the formalisms of Wigner, Skodje, and Truhler,[58,59] were obtained in the temperature range 278−400 K. Small tunneling effect was observed with a transmission coefficient ranging from 1001 to 1040, which implies no effect on the rate constant values calculated in this study. The difference between rate constants obtained at the CBS-QB3 and G3B3 level of theory, in the absence of other studies, cannot be explained and remains a subject of theoretical research; see Figure 5.

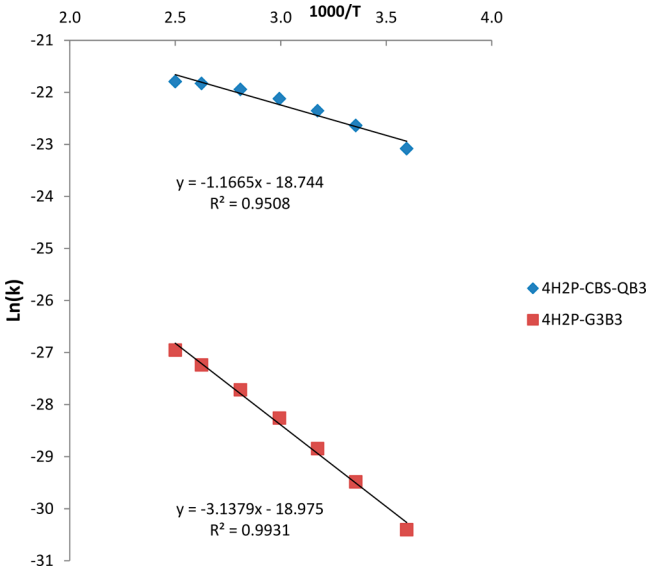

Figure 5. Arrhenius plot $\ln(k)$ versus $1000/T$ for 4H2P + Cl reaction at CBS-QB3 (blue ◆) and G3B3 (red ■).

The previous studies concerning the reactivity of HKs with chlorine atoms have focused on hydroxyacetone $HOCH_2COCH_3$. Kinetic and mechanistic studies of the reaction of hydroxyacetone with Cl atoms have been carried out by Orlando et al.[20] at room temperature using an environmental chamber coupled to a FTIR spectrometry. An average rate constant of 5.6×10^{-11} cm^3 molecule^{-1} s^{-1} was obtained using three different reference compounds (CH_2O, CH_3OH, and C_2H_4). Stoeffler et al.[22] recently studied the same reaction using a relative rate technique over a range of temperature of 281−350 K. This study was carried out using a multipass simulation chamber coupled to a FTIR spectrometer. Rate constants of (4.4 and 6.1) $\times 10^{-11}$cm^3 molecule^{-1}s^{-1} were obtained at 298 K using CH_3OH and CH_3CH_2OH as reference compounds, respectively. However, only the gas-phase reactions of 3H2B and 4H2B with Cl atoms were investigated by Messaadia et al.[21] Sleiman et al.[24] studied the reaction of 3-hydroxy-3-methyl-2-butanone (3H3M2B) with Cl using the relative method that gives a rate constant of 1.13×10^{-10} cm^3 molecule^{-1} s^{-1}.

In a 2017 paper El Dib and coworkers have taken the reaction of 4H4M2P ($CH_3COCH_2C(CH_3)_2OH$) with chlorine; the results give an experimental rate constant of up to 7.4×10^{-11} cm^3 molecule^{-1} s^{-1}. The H atom abstracted on the $-CH_2$ group appeared to be the dominant channel with a small barrier height.[60] The later reactivity can be compared with the one of 4H2P, where the rate constant obtained with the CBS-QB3//B3LYP(6-311G(2d,pd)) at the same temperature is 1.47×10^{-10} cm^3 molecule^{-1} s^{-1}. The difference may be explained by the fact that 4H2P is a linear HK compared with the ramified structure of 4H4M2P. Compared with the 3H3M2B reaction with OH, the ramified structure implies three reaction paths. The path, involving the hydrogen of the methyl adjacent to the hydroxyl group, represents the majority issue with branching ratio equal to ∼52%. For the preferred hydrogen in the CH(OH) group in this study, H abstraction yields a branching ratio of ∼99.99%. It is important to note that hydrogen abstraction is substituted by the methyl in the 3H3M2B and 4H4M2P. In the latter, the theoretical rate obtained gives up to 4.2×10^{-11} cm^3 molecule^{-1} s^{-1} with a branching ratio of 92% in favor of the H abstraction from CH_2 group.[60]

Positive temperature dependence is observed for the reaction of 4H2P with Cl over the temperature range explored where a significant effect of the temperature on the reactivity may be clearly observed.

6. CONCLUSIONS

This study represents the first theoretical determination of the rate coefficient and detailed mechanism for the reaction of Cl atom with 4H2P over the temperature range 278−400 K. This contribution has been carried out using DFT and complete basis set methods (CBS-QB3 and G3B3), exposed as the most efficient and accurate computational methods. The reaction of 4H2P with Cl is exothermic exoergonic and the mechanism is preferentially the H abstraction of the C−H bond from the group −CH(OH) with a branching ratio approaching 100%. The proposed mechanism is supported by the results of El Dib and coworkers for reactions of 3H3M2B and 4H4M2P with chlorine. The rate constant obtained in this study is on the order of those obtained by El Dib and coworkers. The same conclusion can be drawn concerning the 4H2P compared with the 4H4M2P for which theoretical and experimental values are obtained. Positive temperature dependence is observed for the reaction of 4H2P with Cl over the range explored, whereas in the case of 4H4M2P a slight negative temperature effect was observed. The rate constants determined in this study gives a troposphere lifetime of ∼5 to 15 days. This reaction could have a role in the chemistry of the troposphere on local and regional scales.

■ ASSOCIATED CONTENT

Supporting Information

The Supporting Information is available free of charge on the ACS Publications website at DOI: 10.1021/acs.jpca.7b12291.

Geometry Gaussian files in Cartesian coordinates. Table 1. Energies B3LYP/6-311G++(2d,pd), CBS-QB3, and G3B3. Table 2. Relative energies B3LYP/6-311G++(2d,pd), CBS-QB3, and G3B3. Figure 1 Energy profiles obtained using B3LYP/6-31G++(2d,2p)//CBS-QB3 relative enthalpies. Figures 2−5. IRC profiles for 4H2P +Cl. (PDF)

■ AUTHOR INFORMATION

Corresponding Author

*E-mail: azeddine.ferhati@univ-batna.dz; ferhati_azedine@hotmail.com.

ORCID

A. Ferhati: 0000-0001-7430-0207

DOI: 10.1021/acs.jpca.7b12291
J. Phys. Chem. A 2018, 122, 2135−2143

Notes

The authors declare no competing financial interest.

■ ACKNOWLEDGMENTS

We thank MESRS and DGRSDT Algeria.

■ REFERENCES

(1) Matsunaga, S. N.; Wiedinmyer, C.; Guenther, A. B.; Orlando, J. J.; Karl, T.; Toohey, D. W.; Greenberg, J. P.; Kajii, Y. Isoprene oxidation products are a significant atmospheric aerosol component. *Atmos. Chem. Phys. Discuss.* **2005**, *5*, 11143.

(2) Williams, J.; Pöschl, U.; Crutzen, P. J.; Hansel, A.; Holzinger, R.; Warneke, C.; Lindinger, W.; Lelieveld, J. An Atmospheric *Chemistry* Interpretation of Mass Scans Obtained from a Proton Transfer Mass Spectrometer Flown over the Tropical Rainforest of Surinam. *J. Atmos. Chem.* **2001**, *38*, 133.

(3) Lee, Y.-N.; Zhou, X.; Hallock, K. Atmospheric carbonyl compounds at a rural southeastern United States site. *J. Geophys. Res.* **1995**, *100*, 25933.

(4) Zhou, X.; Huang, G.; Civerolo, K.; Schwab, J. J. Measurement of Atmospheric Hydroxyacetone, Glycolaldehyde, and Formaldehyde. *Environ. Sci. Technol.* **2009**, *43*, 2753.

(5) Orlando, J. J.; Tyndall, G. S.; Fracheboud, J.-M.; Estupiñan, E. G.; Haberkorn, S.; Zimmer, A. The rate and mechanism of the *gas*-phase oxidation of hydroxyacetone,. *Atmos. Environ.* **1999**, *33*, 1621.

(6) Stoeffler, C.; Joly, L.; Durry, G.; Cousin, J.; Dumelié, N.; Bruyant, A.; Roth, E.; Chakir, A. Kinetic study of the reaction of chlorine atoms with hydroxyacetone *in* gas-phase. *Chem. Phys. Lett.* **2013**, *590*, 221−226.

(7) Messaadia, L. *Etudes Théoriques et Expérimentales de la Dégradation Atmosphérique des Composés Organiques Oxygénés*. Thesis Cotutelle, University of Batna Algeria/University of Reims, France, 2013.

(8) Thornton, J. A.; Kercher, J. P.; Riedel, T. P.; Wagner, N. L.; Cozic, J.; Holloway, J. S.; Dube, W. P.; Wolfe, G. M.; Quinn, P. K.; Middlebrook, A. M.; Alexander, B.; Brown, S. S. A large atomic chlorine source inferred from mid-continental reactive nitrogen chemistry. *Nature* **2010**, *464*, 271−274.

(9) Aschmann, S. M.; Arey, J.; Atkinson, R. Atmospheric Chemistry of Selected Hydroxycarbonyls. *J. Phys. Chem. A* **2000**, *104*, 3998−4003.

(10) Aschmann, S. M.; Arey, J.; Atkinson, R. Products of the Gas-Phase Reactions of a Series of 1-Alkenes and 1-Methylcyclohexene with the OH Radical in the Presence of NO. *Environ. Sci. Technol.* **2000**, *34*, 1702−1706.

(11) Baker, J.; Arey, J.; Atkinson, R. Rate Constants for the Gas-Phase Reactions of OH Radicals with a Series of Hydroxyaldehydes at 296 ± 2 K. *J. Phys. Chem. A* **2004**, *108*, 7032−7037.

(12) El Dib, G.; Sleiman, C.; Canosa, A.; Travers, D.; Courbe, J.; Sawaya, T.; Mokbel, I.; Chakir, A. Reaction of OH with 4-Hydroxy-2-Butanone (4H2B) at 294 K by Vapor Pressure Measurements of 4H2B. *J. Phys. Chem. A* **2013**, *117*, 117−125.

(13) (a) Messaadia, L.; El Dib, G.; Ferhati, A.; Roth, E.; Chakir, A. Gas phase UV absorption cross-sections for a series of hydroxycarbonyls. *Chem. Phys. Lett.* **2012**, *529*, 16−22. (b) Chia, M.; Schwartz, T. M.; Shanks, B. H.; Dumesic, J. A. Triacetic acid lactone as a potential biorenewable platform chemical. *Green Chem.* **2012**, *14*, 1850−1853.

(14) Cavender, A. E.; Biesenthal, T. A.; Bottenheim, J. W.; Shepson, P. B. Volatile organic compound ratios as probes of halogen atom chemistry in the Arctic. *Atmos. Chem. Phys.* **2008**, *8*, 1737−1750.

(15) Singh, H. B.; Thakur, A. N.; Chen, Y. E.; Kanakidou, M. Tetrachloroethylene as an indicator of low Cl atom concentrations in the troposphere, Geo. *Res. Lett.* **1996**, *23*, 2713.

(16) Spicer, S. W.; Chapman, E. G.; Finlayson-Pitts, B. J.; Plastridge, R. A.; Hubbe, J. M.; Fast, J. D.; Berkowitz, C. M. Unexpectedly high concentrations of molecular chlorine in coastal air. *Nature* **1998**, *394*, 353−356.

(17) Hein, R.; Crutzen, P. J.; Heimann, M. An inverse modeling approach to investigate the *global* atmospheric methane cycle. *Global Biogeochemical Cycles* **1997**, *11*, 43−76.

(18) Lawrence, M. G.; Jockel, P.; vonKuhlmann, R. What does the global mean OH concentration tell us? *Atmos. Chem. Phys.* **2001**, *1*, 37−49.

(19) Priya, A. M.; El Dib, G.; Senthilkumar, L.; Sleiman, C.; Tomas, A.; Canosa, A.; Chakir, A. An experimental and theoretical study of the kinetics of the reaction between 3-hydroxy-3-methyl-2-butanone and OH radicals. *RSC Adv.* **2015**, *5*, 26559−26568.

(20) Orlando, J. J.; Tyndall, G. S.; Fracheboud, J. M.; Estupiñan, E. G.; Haberkorn, S.; Zimmer, A. The rate and mechanism of the gas-phase oxidation of hydroxyacetone. *Atmos. Environ.* **1999**, *33*, 1621−1629.

(21) Messaadia, L.; El Dib, G.; Lendar, M.; Cazaunau, M.; Roth, E.; Ferhati, A.; Mellouki, A.; Chakir, A. Gas-Phase Rate Coefficients for the Reaction of 3-hydroxy-2-butanone and 4-hydroxy-2-butanone with OH and Cl. *Atmos. Environ.* **2013**, *77*, 951−958.

(22) Stoeffler, C.; Joly, L.; Durry, G.; Cousin, J.; Dumelié, N.; Bruyant, A.; Roth, E.; Chakir, A. Kinetic study of the reaction of chlorine atoms with hydroxyacetone in gas-phase. *Chem. Phys. Lett.* **2013**, *590*, 221−226.

(23) Atkinson, R.; Baulch, D. L.; Cox, R. A.; Hampson, R. F.; Kerr, J. A.; Troe, J. Evaluated kinetic and photochemical data for atmospheric chemistry: Supplement III. *J. Phys. Chem. Ref. Data* **1989**, *18*, 881−1097.

(24) Sleiman, C.; El Dib, G.; Ballesteros, B.; Moreno, A.; Albaladejo, J.; Canosa, A.; Chakir, A. Kinetics and Mechanism of the Tropospheric Reaction of 3-Hydroxy-3-methyl-2-butanone with Cl Atoms. *J. Phys. Chem. A* **2014**, *118*, 6163−6170.

(25) Frisch, M. J.; Trucks, G. W.; Schlegel, H. B.; Scuseria, G. E.; Robb, M. A.; Cheeseman, J. R.; Scalmani, G.; Barone, V.; Mennucci, B.; Petersson, G. A.; Nakatsuji, H.; Caricato, M.; Li, X.; Hratchian, H. P.; et al. *Gaussian 09*, revision B.01; Gaussian, Inc.: Wallingford, CT, 2010.

(26) Lee, C.; Yang, W.; Parr, R. G. Development of the Colle-Salvetti correlation-energy formula into a functional of the electron density. *Phys. Rev. B: Condens. Matter Mater. Phys.* **1988**, *37*, 785.

(27) (a) Gonzalez, C.; Schlegel, H. B. An improved algorithm for reaction path following. *J. Chem. Phys.* **1989**, *90*, 2154. (b) Gonzalez, C.; Schlegel, H. B. Reaction path following in mass-weighted internal coordinates. *J. Phys. Chem.* **1990**, *94*, 5523.

(28) Montgomery, J. A.; Frisch, M. J.; Ochterski, J. W.; Petersson, G. A. A complete basis set model chemistry. VI. Use of density functional geometries and frequencies,. *J. Chem. Phys.* **1999**, *110*, 2822.

(29) Coote, M. L.; Wood, G. P. F.; Radom, L. Methyl Radical Addition to CS Double Bonds: Kinetic versus Thermodynamic Preferences. *J. Phys. Chem. A* **2002**, *106*, 12124.

(30) Gutbrod, R.; Schindler, R. N.; Kraka, E.; Cremer, D. Formation of OH radicals in the gas phase ozonolysis of alkenes: the unexpected role of carbonyl oxides. *Chem. Phys. Lett.* **1996**, *252*, 221.

(31) Olzmann, M.; Kraka, E.; Cremer, D.; Gutbrod, R.; Andersson, S. Energetics, Kinetics, and Product Distributions of the Reactions of Ozone with Ethene and 2,3-Dimethyl-2-butene. *J. Phys. Chem. A* **1997**, *101*, 9421.

(32) Fenske, J. D.; Kuwata, K. T.; Houk, K. N.; Paulson, S. E. Formation of the OH Radical in the Reaction of Ozone with Several Cyclo-alkenes. *J. Phys. Chem. A* **2000**, *104*, 7246.

(33) Kroll, J. H.; Sahay, S. R.; Anderson, J. G.; Demerjian, K. L.; Donahue, N. M. Mechanism of HO_x Formation in the Gas-Phase Ozone-Alkene Reaction. *J. Phys. Chem. A* **2001**, *105*, 4446.

(34) Zhang, D.; Lei, W.; Zhang, R. Mechanism of OH formation from ozonolysis of isoprene: kinetics and product yields. *Chem. Phys. Lett.* **2002**, *358*, 171.

(35) Kuwata, K. T.; Templeton, K. L.; Hasson, A. S. Computational Studies of the Chemistry of Syn Acetaldehyde Oxide. *J. Phys. Chem. A* **2003**, *107*, 11525.

DOI: 10.1021/acs.jpca.7b12291
J. Phys. Chem. A 2018, 122, 2135−2143

(36) Fenske, J. D.; Hasson, A. S.; Paulson, S. E.; Kuwata, K. T.; Ho, A.; Houk, K. N. The pressure dependence of the OH radical yield from ozone− alkene reactions. *J. Phys. Chem. A* **2000**, *104*, 7821.
(37) Cremer, D.; Kraka, E.; Szalay, P. G. Decomposition modes of dioxirane, methyldioxirane and dimethyldioxirane—A CCSD (T), MR-AQCC and DFT investigation. *Chem. Phys. Lett.* **1998**, *292*, 97.
(38) Malick, D. K.; Petersson, G. A.; Montgomery, J. A. Transition states for chemical reactions I. Geometry and classical barrier height. *J. Chem. Phys.* **1998**, *108*, 5704.
(39) Stipa, P. The reactivity of aminoxyls towards peroxyl radicals: an ab initio thermochemical study,. *J. Chem. Soc., Perkin Trans.* **2001**, *2*, 1793.
(40) Tiu, G. C.; Tao, T. F. M. Theoretical mechanisms and kinetics of the hydrogen abstraction reaction of acetone by chlorine radical. *Chem. Phys. Lett.* **2006**, *428*, 42−48.
(41) Robinson, P. J.; Holbrook, K. A. *Unimolecular Reactions*; Wiley-Interscience: London, 1972.
(42) Dybala-Defratyka, A.; Paneth, P.; Pu, J.; Truhlar, D. G. Benchmark results for hydrogen atom transfer between carbon centers and validation of electronic structure methods for bond energies and barrier heights. *J. Phys. Chem. A* **2004**, *108*, 2475.
(43) Wood, G. P. F.; Henry, D. J.; Radom, L. Performance of the RB3-LYP, RMP2, and UCCSD (T) procedures in calculating radical stabilization energies for• NHX radicals. *J. Phys. Chem. A* **2003**, *107*, 7985.
(44) Curtiss, L. A.; Raghavachari, K.; Redfern, P. C.; Pople, J. A. Assessment of Gaussian-2 and density functional theories for the computation of enthalpies of formation. *J. Chem. Phys.* **1997**, *106*, 1063.
(45) Baboul, A. G.; Curtiss, L. A.; Redfern, P. C.; Raghavachari, K. Gaussian-3 theory using density functional geometries and zero-point energies. *J. Chem. Phys.* **1999**, *110*, 7650−7657.
(46) Xiu-Juan, Q.; Yong, F.; Lei, L.; Qing-Xiang, G. *Chin. J. Chem.* **2005**, *23*, 194−199.
(47) Samai, S.; Rouichi, S.; Ferhati, A.; Chakir, A. N,N-dimethylformamide (DMF), and N,N-dimethylacetamide (DMA) reactions with NO3, OH and Cl: A theo- retical study of the kinetics and mechanisms,. *Arabian J. Chem.* **2016**, DOI: 10.1016/j.arabjc.2016.10.012.
(48) Roth, E.; Chakir, A.; Ferhati, A. Study of a Benzoylperoxy Radical in the Gas Phase: Ultraviolet Spectrum and $C_6H_5C(O)O_2$ + HO_2 Reaction between 295 and 357 K. *J. Phys. Chem. A* **2010**, *114*, 10367−10379.
(49) Mokrushin, V.; Bedanov, V.; Tsang, W.; Zachariah, M. R.; Knyazev, V. D. *CHEMRATE*, version 1.19; National Institute of Standards and Technology: Gaithersburg, MD, 2002.
(50) Tsang, W.; Bedanov, V.; Zachariah, M. R. Master Equation Analysis of Thermal Activation Reactions: Energy-Transfer Constraints on Falloff Behavior in the Decomposition of Reactive Intermediates with Low Thresholds. *J. Phys. Chem.* **1996**, *100*, 4011.
(51) Knyazev, V. D.; Tsang, W. Chemically and Thermally Activated Decomposition of Secondary Butyl Radical. *J. Phys. Chem. A* **2000**, *104*, 10747.
(52) Knyazev, V. D.; Tsang, W. Isothermal Kinetics at Constant Pressur. *J. Phys. Chem. A* **1999**, *103*, 3944.
(53) Tokmakov, I. V.; Lin, M. C. Reaction of Phenyl Radicals with Acetylene: Quantum Chemical Investigation of the Mechanism and Master Equation Analysis of the Kinetics. *J. Am. Chem. Soc.* **2003**, *125*, 11397.
(54) Tokmakov, I. V.; Lin, M. C. Combined Quantum Chemical/RRKM-ME Computational Study of the Phenyl + Ethylene, Vinyl + Benzene, and H + Styrene Reactions. *J. Phys. Chem. A* **2004**, *108*, 9697.
(55) da silva, G.; Hamdan, M. R.; Bozzelli, J. W. Oxidation of the benzyl radical: mechanism, thermochemistry, and kinetics for the reactions of benzyl hydroperoxide. *J. Chem. Theory Comput.* **2009**, *5*, 3185−3194.
(56) Miyoshi, A. Computational studies on the reactions of 3-butenyl and 3-butenylperoxy radicals. *Int. J. Chem. Kinet.* **2010**, *42*, 273−288.
(57) Galano, A. Isopropylcyclopropane + OH Gas Phase Reaction: A Quantum Chemistry + CVT/SCT Approach. *J. Phys. Chem. A* **2006**, *110*, 9153−9160.
(58) Wigner, E. P. Uber die paramagnetische Umwandlung von Para-Orthowasserstof. *Phys. Chem. B* **1932**, *19*, 203−216.
(59) Skodje, R. T.; Truhlar, D. G. Parabolic tunneling calculations. *J. Phys. Chem.* **1981**, *85*, 624.
(60) Aslan, L.; Priya, A. M.; Sleiman, C.; Zeineddine, M. N.; Coddeville, P.; Fittschen, C.; Ballesteros, B.; Canosa, A.; Senthilkumar, L.; El Dib, G.; Tomas, A. Experimental and theoretical investigations of the kinetics and mechanism of the Cl + 4-hydroxy-4-methyl-2-pentanone reaction. *Atmos. Environ.* **2017**, *166*, 315−326.

DOI: 10.1021/acs.jpca.7b12291
J. Phys. Chem. A 2018, 122, 2135−2143